# Plastic flow equations for the local strain approach in the multiaxial case

C. Madrigal, A. Navarro, C. Vallellano
*Dpto. Ing. Mecánica y Fabricación, Escuela Técnica Superior de Ingeniería*
*Avda. Camino de los Descubrimientos, s/n. 41092, Seville*
*University of Seville*
*navarro@us.es*

**ABSTRACT.** This paper presents a system of plastic flow equations which uses and generalizes to the multiaxial case a number of concepts commonly employed in the so-called Local Strain Approach to low cycle fatigue. Everything is built upon the idea of distance between stress points. It is believed that this will ease the generalization to the multiaxial case of the intuitive methods used in low cycle fatigue calculations, based on hysteresis loops, Ramberg-Osgood equations, Neuber or ESED rule, etc. It is proposed that the stress space is endowed with a quadratic metric whose structure is embedded in the yield criterion. Considerations of initial isotropy of the material and of the null influence of the hydrostatic stress upon yielding leads to the realization of the simplest metric, which is associated with the von Mises yield criterion. The use of the strain-hardening hypothesis leads in natural way to a normal flow rule and this establishes a linear relationship between the plastic strain increment and the stress increment.

**KEYWORDS.** Low cycle fatigue; Plastic Flow Rule; Kinematic Hardening; Non-proportional Loading; Multiaxial Fatigue

## INTRODUCTION

We are trying to develop a theory of cyclic plasticity which allows fatigue designers to make calculations for multiaxial loads in a way as similar as possible to which they do when using the well-known Local Strain methodology for uniaxial low cycle fatigue problems. We would like to define concepts that translate to multiaxial loadings in a simple manner the tools of that trade, namely, the use of the Cyclic Stress-Strain Curve and hysteresis loops, the invocation of the memory rule when hysteresis loops are "closed", the extension of the Neuber or ESED rules to multiaxial loading, etc. We have found it useful to base our theory in the idea of distance between stress points and to calculate these distances by using the expression for the yield criterion [1-6].

The Local Strain Method constitutes nowadays a standard tool for fatigue life predictions in many industries. It has been incorporated in commercial software [7, 8] and it is very well described in textbooks [9, 10]. The extension of the Local Strain Method to the multiaxial case requires at least three main steps. The first one is the development of plastic flow rules which reproduce the way we operate with hysteresis loops, cyclic curves, memory effect and so on in the simple uniaxial case. The second step would be the development of multiaxial Neuber-type rules for dealing with inelastic strains at notches. This relies heavily on the use of a theory of plasticity and hence on the previous step. There are already a

number of proposals in this respect [11, 12]. The third step is probably the most difficult and it is the area where more work has been invested so far: the multiaxial cycle counting and fatigue life criteria. There are too many of them to single any one out. A comparison of several criteria is provided in [13]. They need the stresses and strains as inputs and therefore they also depend on the two previous steps.
We are concerned here with the first step. Our theory does not make use of yield or loading surfaces that move about in stress space, a common ingredient of existing cyclic plasticity theories. It uses the concept of distance in a stress space endowed with a certain metric measurable from the yield criterion. The full mathematical details of the method have been given elsewhere [1-6] and we would just like here to provide a first insight of this idea of distance in the stress space and show some comparison with experimental results. To keep the discussion at the simplest possible level we will restrict the treatment given here to the case of combined tension and torsion loading.

## PLASTIC STRAINS CALCULATIONS

The local strain method revolves around a simplified description of the stress-strain behaviour. A very characteristic feature of the calculations of plastic strains in low cycle fatigue problems is the clear distinction between *loading* and *unloading*. In the uniaxial case, one speaks of loading when the stress goes up in the cycle of applied stress and of unloading when it goes down. During the first quarter of the very first cycle, we "move" along the *cyclic curve* (dashed line in Fig. 1) until unloading starts, marking the first point of load reversal (point A). We then "depart" from the cyclic curve and switch to the hysteresis loop. After a while moving along the descending branch of the hysteresis loop another point of load reversal (point B) will be reached and we will leave the current branch of the loop being traversed and start a new branch going up, and so on. One of the key elements in the simulation of the $\varepsilon-\sigma$ behaviour at a notch for variable amplitude loading is the correct application of the *memory effect* (see [9, chapters 12-14] and [10, chapter 5]), both for closing hysteresis loops and for switching the axes where Neuber's hyperbolas are drawn for each load excursion. This is shown to occur in Fig. 1 as one moves, for example, from point D to point E. After reaching point E the strain is then decreased to point F, following the path determined by the hysteresis loop shape. Upon re-loading, after reaching point E-E', the material continues to point A along the hysteresis path starting from point D, proceeding just as if the small loop E-F-E had never occurred. The same thing happens in the loop B-C-B. As we will point out later on, this memory rule is a simplified representation of the so-called kinematic hardening.

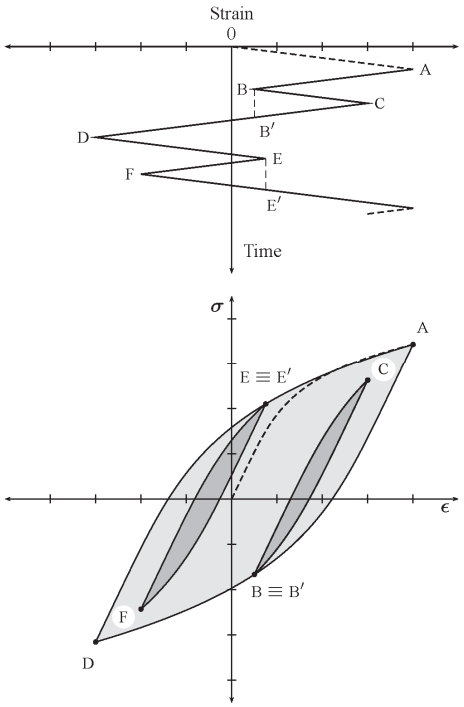


Figure 1: Uniaxial memory effect.

As can be seen, the application of the memory effect depends on a precise control of the distance or separation, in terms of stress, between the successive points of load reversal. Thus, for example, when the stress is descending from C, the memory effect is invoked at B' when the *distance* between the current stress point and C becomes equal to the distance previously established between B and C. Distances between stress peaks and valleys are kept in a stack for comparison and this kind of comparison (at the applied stress level) are really the basis of the cycle counting methods, such as the well-known Rainflow algorithm.

It is not at all clear how we can perform these checks in a multiaxial situation, where some of the components of stress may be increasing while others are decreasing.

The question then is how we reckon distances in the multiaxial case and how we apply the memory effect. We have proposed a way to answer these questions by looking at the yield criterion in a particular way. The development of the theory is still ongoing and the reader interested in the rigorous derivation is directed to [1-6]. To put it in a nutshell, we believe the yield criterion defines the *metric* of the stress space and we show how to obtain all the equations of plasticity from this idea. The metric is the mathematical device that allows one to calculate distances and angles in a vector space, in the stress space in our case. How does it work? First, we treat the stress and strain tensors as vectors, just listing all the components in succession. Let's illustrate the procedure with a relatively simple example. Consider a tension-torsion experiment: a thin-walled cylindrical specimen is subjected to combined tension and torsion under strain controlled conditions. There are only two components of the stress vector $\boldsymbol{\sigma}$ different from zero in this case, the longitudinal stress $\sigma$ and the shear stress $\tau$. Let's assume the material follows the von Mises yield criterion. The Mises yield locus is a circle of radius $\sqrt{2}k$ or $\sqrt{\frac{2}{3}}Y$ in the deviatoric plane, where $k$ and $Y$ denote the yield stresses in pure shear and uniaxial tension (or compression) respectively (see [14, p. 62]). Then, we define the magnitude of the stress vector in the following way, which allows us to say simply that yielding begins when the length or magnitude of the stress vector attains the critical radius

$$|\boldsymbol{\sigma}|^2 = \frac{2}{3}\sigma^2 + 2\tau^2 \tag{1}$$

We notice that we are not using the usual Euclidean norm in Eq. (1), for the coefficients of this quadratic form, which is what it is called the *metric*[1] of the space, are not equal to unity. Mathematically, this signals that our space is not Euclidean, which means, loosely speaking, that the basis vectors are not orthogonal. They form an oblique basis.

We calculate angles between vectors by means of the familiar dot product, but we have to realize that with the metric chosen the rule is a little different from the usual one. Thus for two stress vectors $\boldsymbol{\sigma}_1 = (\sigma_1, \tau_1)$ and $\boldsymbol{\sigma}_2 = (\sigma_2, \tau_2)$,

$$\boldsymbol{\sigma}_1 \cdot \boldsymbol{\sigma}_2 = \frac{2}{3}\sigma_1\sigma_2 + 2\tau_1\tau_2 \tag{2}$$

and the angle $\theta$ between the two vector follows from

$$\cos\theta = \frac{\boldsymbol{\sigma}_1 \cdot \boldsymbol{\sigma}_2}{|\boldsymbol{\sigma}_1||\boldsymbol{\sigma}_2|} \tag{3}$$

What about the plastic strain vector? Do we use the same rule as in the stress case? Not really, because plastic strain components are slightly different. Look at the dot product in Eq. (2). Can we apply this to calculate the plastic work? The result would be:

$$dW_p = \boldsymbol{\sigma} \cdot \boldsymbol{d\varepsilon^p} = \frac{2}{3}\sigma d\varepsilon^p + 2\tau d\gamma^p \tag{4}$$

This is obviously not correct. The plastic work is simply

[1] Eq. 1 is really an integrated form of the metric since the metric is in fact defined in terms of differentials

$$dW_p = \sigma d\varepsilon^p + \tau d\gamma^p \tag{5}$$

How come? Remember the oblique basis business? When we have an oblique basis, we also have a reciprocal basis. The plastic strain components have to do with this *reciprocal basis*. In more precise mathematical terms, stresses and plastic strains behave as *dual vector spaces*. If we have a vector expressed in the original basis and another vector expressed in the reciprocal basis, since the vectors of both bases are, so to speak, orthogonal, then it turns out that their dot product has exactly the form given in Eq. (5). Thus everything is all right. So, finally, how do we calculate the magnitude of plastic strain vectors? One of the nice surprises of the Mises' metric in Eq. (1) is that the rule for calculating the norm of the plastic strain vector turns out to be the usual Euclidean formula:

$$\left|\boldsymbol{\varepsilon}^p\right| = \sqrt{(\varepsilon^p)^2 + \left(\frac{\varepsilon^p}{2}\right)^2 + \left(\frac{\varepsilon^p}{2}\right)^2 + (\gamma^p)^2} = \sqrt{\frac{3}{2}(\varepsilon^p)^2 + (\gamma^p)^2} \tag{6}$$

Please note that in the tension-torsion experiment, while there are only two components of the stress tensor different from zero ($\sigma$ and $\tau$), there are more than two components of plastic strain that must be taken into account, for the hoop and the radial strains are not zero on account of the fact that plastic deformation preserves volume. So if $\varepsilon^p$ is the axial plastic strain, the hoop and radial plastic strains both equal $-\frac{\varepsilon^p}{2}$. This comes out nicely from the general equations given in [2-6].

The usual strain hardening hypothesis, which assumes that the radius of the Mises circle (the so-called equivalent stress) is a function only of the generalized or equivalent plastic strain increment (see [14, p. 68]) now takes the form

$$\left|\boldsymbol{\sigma}\right| = H\left(\int\left|d\boldsymbol{\varepsilon}^p\right|\right) \tag{7}$$

where the integral is taken along the strain path starting at some initial state. $H(\,)$ is a function characteristic of the metal concerned that must be determined experimentally. It is usually a steadily increasing function, for most metals harden when deformed plastically. Under this condition, the function $H(\,)$ has an inverse, $H^{-1}(\,)$ whose derivative $\Phi(\,)$ relates the length of plastic strain vector to the increment of the magnitude of the stress vector

$$\left|d\boldsymbol{\varepsilon}^p\right| = \Phi\left(\left|\boldsymbol{\sigma}\right|\right) d\left|\boldsymbol{\sigma}\right| \tag{8}$$

We call this new function, $\Phi\left(\left|\boldsymbol{\sigma}\right|\right)$ the *hardening modulus*. It can be derived empirically from conventional uniaxial cyclic tests. This rule (8) implies that plastic deformation only occurs when there is a positive increment in the magnitude $\left|\boldsymbol{\sigma}\right|$ of the stress vector $\boldsymbol{\sigma}$. That is, hardening only depends on the increment of the distance. This fact naturally leads to the normality flow rule. Then, the strain increment vector is given by

$$d\boldsymbol{\varepsilon}^p = \left|d\boldsymbol{\varepsilon}^p\right| \boldsymbol{n} = \Phi\left(\left|\boldsymbol{\sigma}\right|\right) d\left|\boldsymbol{\sigma}\right| \boldsymbol{n} \tag{9}$$

where $\boldsymbol{n}$ is the normal unit vector to the yielding surface, i.e., the iso-distance surface in our view, at the stress point. The normal vector is thus given by the gradient of the magnitude $\left|\boldsymbol{\sigma}\right|$ of the stress vector,

$$n_1 = \frac{\partial\left|\boldsymbol{\sigma}\right|}{\partial\sigma} = \frac{2}{3}\frac{\sigma}{\left|\boldsymbol{\sigma}\right|} \tag{10}$$

$$n_2 = \frac{\partial|\boldsymbol{\sigma}|}{\partial\tau} = 2\frac{\tau}{|\boldsymbol{\sigma}|} \tag{11}$$

and it is easy to see that substituting back in (9) we obtain precisely the Prandtl-Reuss equations.
Now, situations where load reversals occur are obviously more complicated. We have found that the definition of distance, or rather separation, between stress points after load reversals, from the point of view of plasticity, must involve the angle formed by the lines joining the current stress point and the point of load reversal and this with the origin. However, given the introductory nature of this presentation, this will not be discussed here further. The reader is kindly directed to our last publication [6] to see how this leads to an alternative representation of kinematic hardening and how a multiaxial memory rule can be defined in a rather intuitive way. The flow equations derived can be seen to involve explicitly the points of reversal in each loading segment and there is no need to use yield surfaces moving around in stress space. Everything is controlled by distance.

## APPLICATION TO EXPERIMENTAL RESULTS

This section discusses the application of the proposed model to experimental results reported by Lamba and Sidebottom [15] on a tubular specimen of oxygen-free high-conductivity (OFHC) copper subjected to combined tension and torsion. The specimen was used for investigating the subsequent strain hardening behaviour after shear strain cycling through the strain control program shown in Fig. 2. The cyclic path sequence was 0-1-0-1-0-2-0-2-etc. All paths started at the crossing point, in the left top corner of the figure. Prior to this strain history the specimen had been cycled under shear strain control until it cyclically stabilized and then along a 90° out-of-phase path until it re-stabilized. A comparison made between uniaxial and out-of-phase hardening cycling showed that the cyclic hardening produced by out-of-phase cycling was appreciable greater.

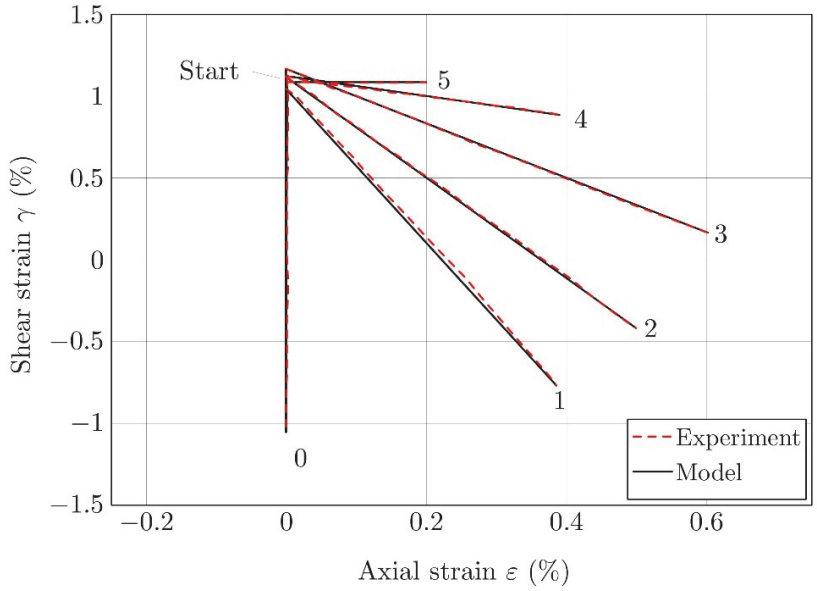


Figure 2: Imposed strain history for the subsequent strain hardening experiment. (The cyclic path sequence was 0-1-0-1-0-2-0-2-etc).

This experiment was employed by Lamba and Sidebottom [15] to show the erasure of memory effect observed if the material had been stabilized by 90° out-of-phase strain cycling. According to the authors, as long as the subsequent strain paths remain in the region enclosed by the out-of-phase cycling, one "big" strain cycle with the same or slightly lesser maximum strain as that imposed for the out-of-phase cycling always brings the material to one particular plastic state. The importance of this observation is that the entire strain hardening behaviour can be studied with just one specimen as long as it is subjected to one "big" cycle between each pair of strain paths.

The stress-strain response to the path in Fig. 2 appears in Fig. 3, along with the predicted results. In the calculations reported here only the path sequence in Fig. 2 has been considered. The out-of-phase hardening has been taken into account by obtaining the model parameters, namely the metric constants and the hardening modulus function from the stress response and from the stable effective cyclic stress-strain curve derived in a 90° out-of-phase experiment, respectively.

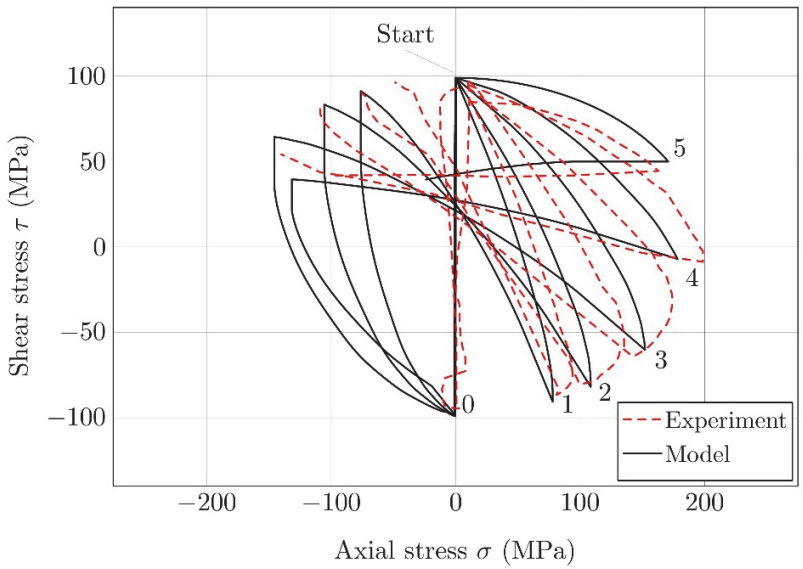


Figure 3: Stress response to strain path in Fig. 2.

The model predictions quantitatively agree with the experimental results. The strain and stresses at the end of each path are shown in Tab. 1, along with the model predictions. The model's average error is around 7,5 %, which is much lower than similar studies reported in the literature [16, 17].

| | Strain Path | | Experimental Results | | Model Predictions | | | | | |
|---|---|---|---|---|---|---|---|---|---|---|
| Point | $\varepsilon$ (%) | $\gamma$ (%) | $\sigma$ (MPa) | $\tau$ (MPa) | $\sigma$ (MPa) | Error (MPa) | Error (%) | $\tau$ (MPa) | Error (MPa) | Error (%) |
| 0 | 0.0 | -1.1 | 0.0 | -94.5 | 0.0 | - | 0.0 | -98.8 | 4.3 | -4.6 |
| 1 | 0.4 | -0.8 | 80.9 | -86.7 | 77.9 | 3.0 | 3.7 | -90.5 | 3.8 | -4.4 |
| 2 | 0.5 | -0.4 | 99.7 | -80.5 | 108.5 | -8.8 | -8.9 | -81.9 | 1.4 | -1.7 |
| 3 | 0.6 | 0.2 | 142.4 | -64.2 | 152.2 | -9.8 | -6.9 | -60.3 | -4.0 | 6.2 |
| 4 | 0.4 | 0.9 | 198.6 | -8.8 | 178.2 | 20.4 | 10.3 | -7.1 | -1.6 | 18.6 |
| 5 | 0.2 | 1.1 | 162.9 | 44.3 | 170.7 | -7.8 | -4.8 | 49.9 | -5.6 | -12.6 |

Table 1: Comparison of experimental results and model predictions.

## ACKNOWLEDGEMENTS

The authors would like to thank the Spanish Ministry of Education for its financial support through grant DPI2014-56904-P.

## REFERENCES


[1] Navarro, A, Brown, M.W., Miller, K.J. J., A multiaxial stress-strain analysis for proportional cyclic loading, Strain Anal. Eng., 28 (1993) 125-133.

[2] Navarro, A., Brown M.W., A constitutive model for elasto-plastic deformation under cyclic multiaxial straining, Fatigue Fract. Eng. Mater. Struct., 20 (1997) 747-758.

[3] Navarro, A., Plastic flow and memory rules for the local strain method in the multiaxial case, In: Susmel L., Tovo R., (Eds)., Progettazione a Fatica in presenza di Multiassialità Tensionali, Proceedings of the IGF workshop, Ferrara, (2005)

[4] http://www.gruppofrattura.it/ocs/index.php/gigf/gigf2005/schedConf/presentations.

[5] Navarro, A., Giráldez, J.M., Vallellano, C., A constitutive model for elastoplastic deformation under variable amplitude multiaxial cycling loading, Int. J. Fatigue 27 (2005) 838-846.

[6] Madrigal, C., Navarro, A., Chaves, V., Numerical implementation of a multiaxial cyclic plasticity model for the local strain method in low cycle fatigue, Theor. Appl. Fract. Mech., 80 (2015) 111-119.

[7] Madrigal, C., Navarro, A., Chaves, V., Biaxial cyclic plasticity experiments and application of a constitutive model for cyclically stable material behaviour, Int. J. Fatigue, 83 (2016) 240-252.

[8] MSC.Fatigue, MSC Software Corporation.

[9] FE-Fatigue, nCode International.

[10] Dowling, N.E., Mechanical Behaviour of Materials. Engineering Methods for Deformation, Fracture and Fatigue, Prentice Hall, Inc., Englewood Cliffs, NJ, (1993).

[11] Bannantine, J.A., Comer, J.J., Handrock, J.L., Fundamentals of Metal Fatigue Analysis, Prentice Hall, Inc., Englewood Cliffs, NJ, (1990).

[12] Hoffman, M., Seeger, T.A., A generalized method for estimating multiaxial elastic-plastic notch stresses and strains, Part 1: Theory, J. Eng. Mater.-T. ASME, 107 (1985) 250-254.

[13] Glinka, G., Buczyński, A., Ruggeri, A., Elastic-plastic stress-strain analysis of notches under non-proportional loadings paths, Arch. Mech., 52 (2000) 589-607.

[14] Socie, D.F., Marquis, G.B., Multiaxial Fatigue, Society of Automotive Engineers, Inc., Warrendale, PA, (2000).

[15] Chakrabarty, J., Theory of Plasticity, 3rd ed., Elsevier Butterworth-Heinemann, Oxford, (2006).

[16] Lamba, H.S., Sidebottom, O.M., Cyclic plasticity for nonproportional paths: Part 1 – Cyclic hardening, erasure of memory, and subsequent strain hardening experiments, J. Eng. Mater. Technol., 100 (1978) 96-103.

[17] McDowell, D.L., Socie, D.F., Lamba, H.S., Multiaxial nonproportional cyclic deformation, ASTM STP, 770 (1982) 500-518.

[18] Lamba, H.S., Sidebottom, O.M., Cyclic plasticity for nonproportional paths: Part 2 – Comparison with predictions of three incremental plasticity models, J. Eng. Mater. Technol., 100 (1978) 104-111.